Polymer 51 (2010) 5780–5787

Contents lists available at ScienceDirect

Polymer

journal homepage: www.elsevier.com/locate/polymer

Morphology of undeformed and deformed polyethylene lamellar crystals

A. Galeski [a,*], Z. Bartczak [a], T. Kazmierczak [a,1], M. Slouf [b]

[a] Centre of Molecular and Macromolecular Studies, Polish Academy of Sciences, Sienkiewicza 112, 90363 Lodz, Poland
[b] Institute of Macromolecular Chemistry, Czech Academy of Sciences, Heyrovskeho nam. 2, 162 06 Praha 6, Czech Republic

ARTICLE INFO

Article history:
Received 28 July 2010
Received in revised form
30 September 2010
Accepted 1 October 2010
Available online 12 October 2010

Keywords:
Polyethylene
Lamellae
Plastic deformation

ABSTRACT

Morphology of undeformed polyethylene crystals obtained by high pressure crystallization was investigated by SEM. It was revealed by exposing the interior of the samples by microtoming followed by permanganic etching. The etching procedure was refined to reveal defected sites of lamellae in addition to differentiation of crystalline and amorphous phases. From 1 to 3 screw dislocations with large Burgers vector per 1 μm^2 of lamellae basal planes were detected. Lamellae, when viewed edge-on give an impression of a "blocky architecture", while their real shape, as seen on SEM images of flat-on and oblique lamellae, resembles platelets with a few defects in the form of screw dislocations protruding a platelet.

High pressure-crystallized polyethylene samples were deformed plastically by uniaxial compression and were studied by SEM and AFM. When the deformation is interrupted dislocations are arrested within the crystals. It was observed that in contrast to undeformed samples, the side faces of deformed lamellae were not any longer smooth and a large number of screw dislocations with low Burgers vectors crossing the lamellae thickness could be distinguished. These observations are in accordance with polymer crystal plasticity theory that relies on the rate controlled nucleation and propagation of screw dislocations across polymer crystals. An existence of numerous screw dislocations arrested in lamellae is a direct proof of action of fine crystallographic slips along the macromolecular chains in PE crystals during plastic deformation. The kinking of lamellae due to plastic deformation was also observed. Large sections of lamellae between kinks rotated towards the plane of compression while the chain stems in lamellae rotated in the opposite direction, away from the compression direction, which is a signature of the fine crystallographic slip.

Plastically deformed polyethylene crystals are highly defected due to many dislocations incorporated within them – the density of dislocations was approximated as 10^{16} m^{-2}. However, deformed crystal melting temperature is nearly unaffected while the heat of melting is slightly reduced, yet only in thin crystals. It suggests that the arrested dislocations contribute more to the surface energy of lamellae basal planes rather than to a bulk energy of polyethylene crystals.

1. Introduction

In 1949 Frank et al. [1,2] suggested that the faster growth of crystals could take place due to formation of screw dislocations. Consequently, any real crystal should contain a number of dislocations with a screw component, terminating on the face. Crystallization of any substance is always easier, if screw dislocations are engaged, due to a dihedral angle benefit. The theory of crystal growth based on dislocation theory as formulated by Frank [2] predicted the presence of growth features in the form of flat, spirally terraced hills on the crystal face perpendicular to a screw dislocation line and centered on it. The height of a terrace step should be equal to the Burgers vector of the dislocation, usually just one unit of a crystallographic cell. In fact, that prediction was confirmed many times by various experimental techniques. The observed density of dislocations varies widely on different specimens and different low molecular weight materials, ranging from a few thousands (whiskers) up to about 10^9–10^{12} m^{-2} (polycrystalline metals) [3].

Crystallization of polymers is also prompted by screw dislocations. Screw dislocation growth mechanism in polymer single crystals has been reported since long time [4–6], see also monographs [7,8]. However, the few direct experimental observations of dislocations in polymer crystals were done mostly in solution-grown polymer single crystals so far [9,10]. Dislocations in samples crystallized from the melt were detected only occasionally [11,12].

* Corresponding author.
E-mail addresses: andgal@cbmm.lodz.pl (A. Galeski), bartczak@cbmm.lodz.pl (Z. Bartczak), slouf@imc.cas.cz (M. Slouf).
[1] Present address: ABB Corporate Research Centre, Cracow, Poland.

0032-3861/$ – see front matter © 2010 Elsevier Ltd. All rights reserved.
doi:10.1016/j.polymer.2010.10.004

Even a very conservative estimate of the number of dislocations existing in polymer crystals, gives their density in the range of 10^9–10^{12} m^{-2} [13]. The lower-bound estimate corresponds to few dislocations per μm^2 of the lamellae basal plane. On the basis of TEM study Peterman and Gleiter estimated the dislocation density in solution-grown polyethylene single crystals at around 10^{12}–10^{14} m^{-2} [9]. Dislocation density in melt-crystallized polypropylene, estimated experimentally on the basis of X-Ray diffraction profile analysis, is much higher, approximately 2×10^{16} m^{-2} [14], which is a few orders of magnitude larger than in low molecular materials. In terms of the introduction of screw dislocations during crystal growth, Schultz and Kinloch [15] and Schultz et al. [16] presented a model calculation of the twisting correlation of crystallites in a banded spherulite (a spherulite showing periodic extinction bands under polarizing optical microscope) with the row of screw dislocations of the same handedness. Based on their argument, Hikosaka et al. [17] postulated a possibility of the twisting correlation due to introduction of the selective screw dislocations in the chair type PE crystals for the formation of banded spherulites. Recently, Ikehara et al. [18] showed by 3D electron tomography, apparently searching for so-called "giant" screw dislocations, that no such screw dislocations are engaged in the formation of banded spherulites of PCL/PVB blends. Nevertheless, the existence and a significant role of screw dislocations in melt-crystallized polymers was quite well established (see e.g. Refs. [14,19,20]).

The so-called "giant" screw dislocations observed in single crystals of polymers may have the Burgers vector extraordinarily large, up to 10 nm or more, being equal to the total thickness of lamellar crystals [13,21]. Such dislocations are easily detectable by microscopy, yet observations demonstrated that they did not show hollow cores as would be required for such large dislocations in most of materials. In polymer lamellae the axes of giant screw dislocations are parallel to the molecular stems. Such dislocations must involve a readjustment in chain folding on a large scale in order to avoid formation of holes. As a consequence the "giant" dislocations become immobile. During crystallization they appear sporadically at growth fronts, especially at points of chain reentering. The "giant" screw dislocations play a vital role in lamellar branching and in morphological development of radiating polycrystalline aggregates [13]. Spatial constraints arising during formation of giant dislocations stimulates adjacent lamellae to develop similar dislocations – the phenomenon is often observed in stacks of lamellae. The role of giant dislocations in crystallization by chain folding was already recognized many years ago (see, for example, a review in the Geil's book [7] and a discussion on dislocations in polymer crystals in Ref. [22]).

Dislocations are also very important for plastic deformation of crystalline polymers. The model developed by Young [23,24], invokes the classical theory of crystal plasticity to plastic deformation of polymers. In that approach it is expected that the plastic deformation of polymer crystals, like plastic deformation of crystals of other materials, is crystallographic in nature and takes place by crystallographic slip mechanism, without destroying the crystalline order. The slip mechanism is governed by the generation and movement of dislocations along the slip plane. There is a vast experimental evidence that in absence of voiding the deformation of polymer crystals occurs primarily by slip mechanism, similar to the slip processes observed in metals, ceramics or other low molecular weight crystals (see e.g. the reviews [25–27]). In this slip mechanism the nucleation of dislocations and their motion across slip planes play a primary role.

The amount of mobile dislocations that is already present in polymer crystals is usually not sufficient to initiate their plastic deformation. The current view on the processes is that beyond the yield point many more new screw dislocations are generated at crystal edges and propagate through the crystal. It has been shown that screw dislocations parallel to the chain stems may be easily nucleated from the lateral surface of thin polymer crystal platelets upon coupled thermal and stress activation [23,24,28,29]. An emission of dislocations from the edges of the lamellae across the narrow faces as a thermal nucleation process was initially proposed by Peterson [28,29], explored further by Shadrake and Guiu [30] and more rigorously by Young [24]. This mechanism is currently widely accepted [14,25,26,31]. The model of thermal nucleation of screw dislocations [23,24,28,29] was demonstrated to account fairly well for the plastic behavior of polyethylene (PE) [32,33] and polypropylene (PP) [32] and for the yield stress dependency on the crystal thickness [35,36]. Elastic line energy calculations indicated that nucleation of screw dislocations is more favorable than of edge dislocations [30,37]. The glide is also easier for the former [38]. The activation volume of dislocation emission was determined from strain rate jump experiments during uniaxial compression of PE [31]. The mean activation volume was of the order of 350 of crystallographic unit cells and the estimated typical radius of the dislocation was 3.8 nm [31]. This indicates that the Burgers vector of such thermally generated dislocation must be small, of order of few lattice units only, i.e. much smaller than that of immobile "giant" dislocations formed sporadically during crystal growth. Apparently, the dislocations of such characteristics are the easiest to generate. It is then logical to assume then that easy to detect "giant" dislocations constitute only a small fraction of screw dislocations arising on melt crystallization of polymers while the most of dislocations formed have similar characteristics to those generated thermally upon deformation, i.e. have short Burgers vector and are highly mobile. On the other hand, it is known that even a light annealing of crystals of low molecular weight materials causes the dislocations to migrate towards crystal edges and then disappear [39]. That migration is faster and easier for dislocations with smaller Burgers vector. Similar behavior can be expected for dislocations in polymer crystals: for long crystallization time or prolonged annealing only dislocations with large Burgers vector, including immobile "giant" screw dislocations would remain in polymer crystals, while most of those with low Burgers vector, exhibiting higher mobility, would leave polymer lamellae.

The aim of this communication is to demonstrate the incorporation of screw dislocations within polymer crystalline lamellae grown from the melt, as well as within plastically deformed lamellae, and additionally to illustrate the implications of their presence on the observed morphology. For this purpose we have chosen high density polyethylene crystallized under pressure. Crystallization of PE under high pressure yields usually lamellae notably thicker than crystallization at low pressure. That feature makes the microscopic observations much easier.

Earlier investigations of thick PE crystals crystallized under high pressure showed that the chains are not fully straightened. Only short chains demonstrate full extension [40], while longer chains are still partially folded unless they are located in the so-called type III lamellae [41,42]. Further studies of the morphology of thick crystals obtained at various crystallization conditions showed that full chain extension is rather an exception than a rule [43]. Crystals thicker than the chain length are formed by incorporation of chain ends within crystals. Other similarities between crystals formed at high pressure and crystals formed at atmospheric pressure led to the conclusion that crystals formed at high pressure are enlarged copies of folded crystals [44].

We have refined the permanganic etching procedure [45,46] in order to distinguish the defected fragments of lamellae containing dislocations from fragments characterized by perfect crystalline lattice, in addition to differentiation between crystalline and amorphous phases.

2. Experimental

2.1. Samples

High density polyethylene (HDPE) was used in this study (Lupolen 5280HX; BASF; M_w~120,000, M_w/M_n~3.4, density 0.952 g/cm^3, MFI of 2.3 g/10 min at 190 °C/2.16 kg). Since this experimental grade polymer was supplied without additives, additional stabilizers and antioxidants were added to prevent excessive oxidation of polyethylene during processing and crystallization: a mixture of 0.1 wt.% of Irganox 1010 and 0.2 wt.% of Irgafos 168 was dry blended with the polyethylene powder prior to melting and extruding in the form of rods 9.5 mm in diameter. In order to grow thick lamellae for easier morphology investigations the samples were crystallized at high pressure, varied in the range of 450–630 MPa, in a pressure cell consisting of a barrel with two pistons, and a loading frame of the tensile testing machine (Instron 5580). The computer control of the loading frame allowed to maintain the constant hydrostatic pressure inside the cell with an accuracy of 0.2 MPa. Depending on pressure the crystallization temperature was selected from the range of 235–257 °C. The temperature of the sample in the cell was controlled with an accuracy better than 0.5 °C. Various conditions of crystallization (pressure, temperature) were applied in order to obtain samples of different crystallinity and containing crystals of different thickness. Samples in the form of cylindrical rods 9.5 mm in diameter were placed in the pressure cell, heated to the desired temperature and then pressurized. Samples were kept at that temperature and pressure for a period of time, usually 1 h, for completion of crystallization. Then the cell with a sample inside was cooled down to room temperature and the pressure released. Details of the high-pressure cell and experimental procedure are given elsewhere [31].

2.2. Uniaxial compression

Specimens crystallized at high pressure were deformed in uniaxial compression. This deformation mode was chosen since produces the state of stress that does not promote any unwanted cavitation of the deformed material. The specimens in the form of tablets 3 mm high and 9.5 mm diameter were carefully machined out of the cylindrical samples of high pressure-crystallized PE. They were subjected to uniaxial compression in a universal tensile testing machine (Instron, Model 5582). The compression platens of the compression fixture were polished and additionally lubricated. All compression tests were performed at room temperature and a constant true strain rate of 0.0005 s^{-1}, 0.005 s^{-1}, 0.05 s^{-1} or 0.5 s^{-1}.

2.3. Etching and microscopy

The specimens for morphological observations were cut off from the high-pressure-crystallized samples using a fine saw or a sharp blade. Final smooth surfaces appropriate for etching were revealed by cutting with ultramicrotome and a freshly prepared glass knife or a diamond knife, at room temperature. The top layer, possibly deformed plastically during sectioning was etched out and the bulk morphology of the samples was exposed by further etching in a permanganic etchant mixture at room temperature according to the procedure developed originally by Bassett et al. [45,46] and refined by us for the application to the high pressure-crystallized HDPE. The best results were obtained for etching in the mixture of H_2SO_4, H_3PO_4 and $KMnO_4$ of the composition 1 vol.:1 vol.:1 wt.% of total weight, for 30 min. To improve etching the mixture was placed in an ultrasonic bath running periodically for short time periods during the etching process. The etching was stopped and the specimens were washed subsequently in four washing baths as follows: (1) cold (from a fridge) diluted H_2SO_4 (2 volumes H_2SO_4:7 volumes of distilled water), (2) concentrated H_2O_2 (30%) from the fridge, (3) distilled water and (4) acetone. The washing baths were placed in an ultrasonic bath. Washing in each bath was for at least 2 min.

The 30 min etching time was chosen on the basis of a series of trial experiments at room temperature. Longer etching times (1 h and 2 h) did not improve the results. Therefore, the shortest time of 30 min was used to minimize the risk of artifacts due to an over-etching. Also the composition of the etching mixture was optimized on the basis of prior experiments with a range of mixtures of various compositions.

Etched, washed accordingly and dried specimens were coated with fine gold layer by ion-sputtering (JEOL JFC-1200) and examined with a scanning electron microscope (JEOL JSM-5500LV) operating in the high vacuum mode at accelerating voltage of 10 kV.

Interior of uniaxially compressed samples was exposed by microtoming with an AFM diamond knife (Diatome) along the direction of compression and then etched according to the procedure described above. The time of etching was shortened to reveal the details of the morphology, yet not to produce excessive roughness. Etched surfaces were examined using Atomic Force Microscope, Nanoscope IIIa (Digital Instruments) or SEM (after coating with gold).

2.4. DSC

Thermal analysis was conducted using a TA 2920 DSC apparatus (Thermal Analysis). The melting thermograms were recorded at the heating rate of 10 °C/min, under nitrogen flow. The crystallinity level and the length of the crystalline stem, l^*, which is close to the lamellar thickness, were estimated on the basis of the heat of melting of the sample recorded during heating and from the recorded melting temperature, T_m, respectively. The precision of melting peak assessment was better than 0.5 °C. For the determination of the heat of melting a baseline was approximated in a standard way with a straight line aligned with the signal line at temperatures above the melting peak. An approximate range of the integration was between 60 and 155 °C. For the estimation of l^* the following equation was used [47]:

$$l^* = \frac{2\sigma_e T_m^0}{\Delta h_f \left(T_m^0 - T_m\right)} \quad (1)$$

where σ_e is the lamellar basal surface free energy (for PE $\sigma_e = 9 \times 10^{-6}$ J/cm^2 [48], Δh_f is the heat of fusion per unit volume (for PE $\Delta h_f = 293$ J/cm^3 [49], $T_m^\circ = 145.1$ °C is the extrapolated equilibrium melting temperature determined earlier by us [50] for polyethylene used in this work.

2.5. Raman spectroscopy

Low acoustic frequency Raman spectra of PE samples were recorded by means of a high resolution Raman Spectrometer Z40 (DILOR) equipped with 5 diffraction grids. The light source was a 120 mW argon laser ($\lambda = 514.5$ nm).

3. Results

A range of polyethylene samples with different crystallinity and thickness of lamellae was prepared by crystallization at high pressure. A representative sample, crystallized under pressure of 488 MPa and at temperature of 245 °C, presented in Fig. 1, is

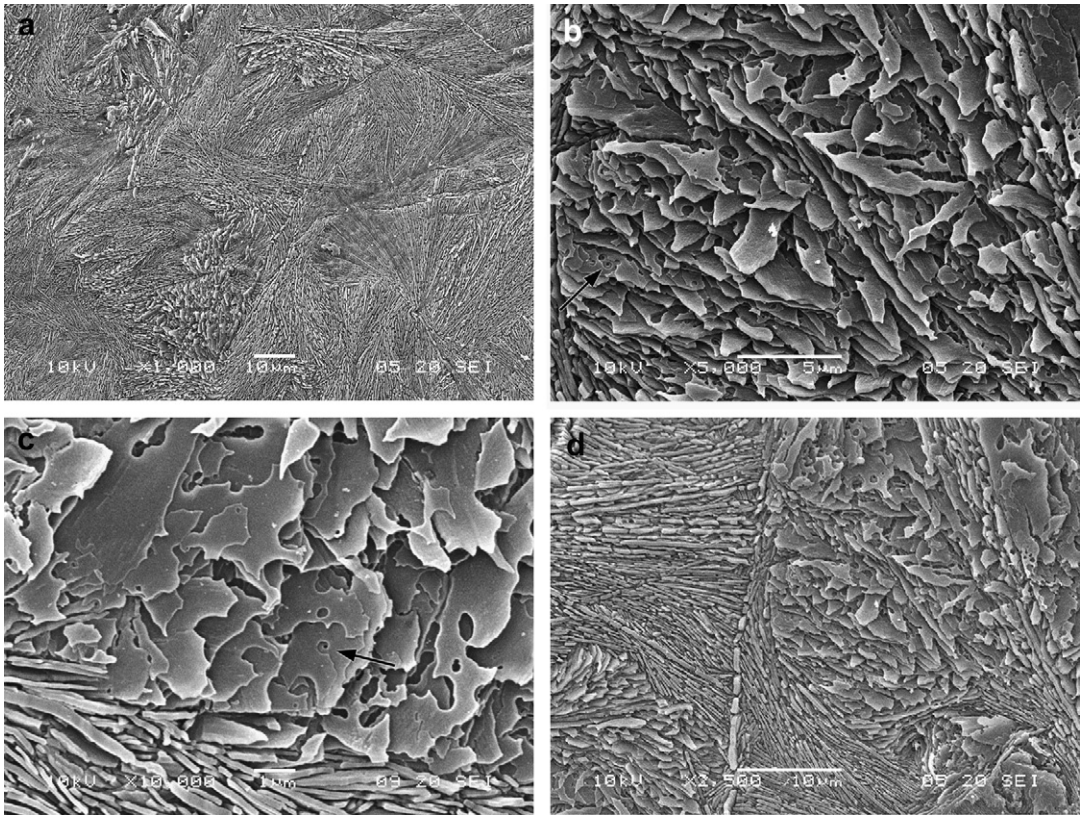

Fig. 1. SEM micrographs of bulk HDPE crystallized at high pressure ($p = 488$ MPa, $T = 245$ °C) to grow thick lamellae for better visualization. Sample was cut with a glass knife and etched. (a) Overview, (b) details showing flat lying lamellae, (c) details of a sample with helically twisted giant dislocations and (d) details showing edge-on lamellae.

characterized by the peak melting temperature of 143.1 °C, that corresponds to a mean lamellae thickness l^* of around 130 nm. Comparing with the number average length of fully extended PE macromolecules that is around 320 nm, it can be concluded that the chains can not be fully extended within crystals and must fold several times, so these crystals can be classified as "chain extended" rather than "extended chain". The heat of melting is 263.2 J/g which corresponds to the crystallinity degree of 90%. Similar value of crystallinity was obtained from wide angle X-ray diffraction data. The small angle X-Ray scattering pattern, recorded with a camera having the resolution up to 40 nm, shows a very weak scattering, resembling a tail of a possible peak located at very low diffraction angle which was actually obscured by the beam stop. Such a pattern might indicate a presence of thick crystals ($l^* > 40$ nm) which scatter X-ray at very low angles. Also the low frequency longitudinal acoustic emission in Raman spectrometer does not show any peak; apparently the crystals are too thick to produce low frequency signal that can be detected by the high resolution Raman spectrometer.

Exemplary SEM images of the exposed interior of the high pressure-crystallized PE sample are presented in Fig. 1a–d. In a low magnification SEM picture shown in Fig. 1a a rough spherulitic arrangement of crystalline elements can be recognized. An analysis of the features of the revealed morphology led to the conclusions that etching procedure exposed lamellar structure of the material, as expected. The lamellae are approximately 100–300 nm thick and tens of micrometers wide and long. The edges of crystalline lamellae are sharp while the faces are flat and smooth. As can be observed at higher magnification (cf. Fig. 1b and c) the flat-on oriented lamellae show occasionally round holes, approximately 1–3 holes per 1 μm^2 at average. These holes are the result of selective etching of the material of apparently lower perfection, more susceptible for etching than surrounding crystalline matter, similarly to the etch pits around dislocations which can be produced and observed in low molecular crystals. In the interior of some of such holes a screw architecture can be observed (see e.g. the center of Fig. 1c or the middle of left edge of Fig. 1b, indicated with arrows; also the right edge and the top of that micrograph contain such morphological details). Evidently, they must be some remnants after etching of most of the material from the vicinity of screw dislocations with rather large Burgers vector, possibly exceeding the thickness of a single lamellae. Those can be classified as "giant" screw dislocations described by Keith et al. [13]. The other holes, without clear screw architecture, in our opinion, are most probably located in places where screw dislocations with smaller Burgers vectors were present before etching. These are more numerous than spiral holes visualizing "giant" dislocations. The material around screw dislocation lines is apparently etched faster than a not defected crystalline surrounding because of the stress due to distortion of crystalline lattice in the proximity of the dislocation line, similarly to etch pits which can be produced in low molecular crystals around dislocation lines. Apparently the size of etched holes around screw dislocations is related to the extent of that distortion and hence, to the magnitude of the Burgers vector. It is clear then that these screw dislocations are characterized by various Burgers vector, some as low as few lattice unit cells, that result in the round pits or small holes etched across the thickness of lamellae.

However, when the lamellae of the same sample are viewed edge-on the picture seems to be completely different: the pattern produced by selective etching around screw dislocation makes an impression of fragmented lamellae built from "shingles"(cf. left-hand side of image in Fig. 1d). We interpret the discontinuities observed on lamella edges in the edge-on projection as semi-round

holes etched around dislocation line, identical to those seen in flat-on lamellae, but now viewed in the perpendicular, cross-section projection. For sure, any of such discontinuities does not extend much deeper below the plane of observation, i.e. does not divide the lamella into separate blocks (this can be seen clearly in lamellae viewed in an oblique projection). Such a discontinuous shingle-like pattern observed in edge-on oriented lamellae, however, resembles very much the "blocky structure" observed in the past with AFM by other researchers [51,52]. The matter associated with the screw dislocation is softer than non-defected regions of the crystal, hence it is more susceptible to etching than a perfect crystals. At the same time these defects, being softer than the surrounding perfect crystal matter, can be sensed and visualized in AFM tapping mode creating an artificial image of separate blocks aligned along the line of lamella. We believe, that the discontinuous morphology of lamellae observed with AFM in a tapping mode by Hugel, Strobl and Thomann [51] and interpreted as the "blocky structure" might be related to this feature of defected crystal rather than to the real discontinuity of lamellar crystals. In our view the difference in length of "shingles", from 0.5 to 5 μm, and "blocks" observed in [51,52], from 20 to 30 nm, results from densities of dislocations: our undeformed samples were crystallized very slowly (2–3 h) and most of dislocations diffused outside crystals. The density dislocations is then 2 per μm^2, that gives $2 \times 10^{12}/m^2$ while X-ray line profile studies gives for melt-crystallized polyethylene samples $2 \times 10^{16}/m^2$ [14]. That explains the difference in distances between dislocations and hence, the difference in sizes of "shingles" and "blocks".

Crystallization of PE under high pressure involves a great deal of annealing (crystallization at high pressure requires high temperature, 230–260 °C, and long time, 1–3 h) and there was a great chance for many screw dislocations formed during crystal growth to diffuse to the lamellae edges and then out of the crystal. Nevertheless, as evidenced by micrographs about 1–3 dislocations per μm^2 of lamellae basal planes, including those immobilized giant dislocations of very large Burgers vectors, preserved annealing and still remained inside crystals. It could be speculated that any hypothetical "blocky structure", if existed at the growth stage, was also fused in a similar way due to prolonged annealing. However, we were not able to detect any remnant or the slightest trace of that structure in thick polyethylene lamellae.

The picture of thick polyethylene lamellar crystals that emerges from the above reported microscopic observations is a flat solid plate with isolated line defects protruding the plate. Although these conclusions are drawn for thick crystals of high density polyethylene obtained at high pressure, they should hold also in conventional thin lamellar crystals grown during crystallization at low pressure. This envision is based on well established concepts: nucleation, crystal growth and screw dislocations augmenting the crystallization. It offers another, simpler explanation of the impression of "blocky structure" of crystalline lamellae observed in the past with AFM [51,52] than that offered previously, based on the hypothesis of subsequent steps of lamella growth [51].

As it was outlined in the Introduction, plastic deformation of polymer crystal involves a generation of many new screw dislocations at crystal edges and their travel across crystals under the action of the shear stresses (slip mechanism). While some dislocations travel out and leave the crystal, new dislocation are nucleated. It is believed that there is a certain dislocation concentration generated and then maintained in a deforming crystal that is adjusted to the applied strain rate and the temperature of deformation [31,53]. When the deformation is interrupted all dislocations become arrested at their momentary positions. The structure of sheared crystals must be different than that of pristine crystals not subjected to shearing: while pristine lamellae contain relatively low number of dislocation, including a fraction of immobile "giant dislocations" of very large Burgers vector (10^6 m^{-2}; see above), the deformed lamellae should contain many more of arrested dislocations, yet having mostly low Burgers vectors, as those are preferred by the mechanism of thermal nucleation [24,31].

Fig. 2a presents SEM micrograph illustrating the etched side faces (edges) of thick pristine PE lamellae. It is seen that these side faces are very smooth and exhibit only occasional etch pits or holes – remnants of etched screw dislocation (N.B. note the wedge shape of some pits, illustrating partial etching). The smoothness of side faces of lamellae that is seen on Fig. 2 demonstrates that distorted layer of the material formed during cutting was completely removed by etching. The intact pristine lamellae are characterized by nearly perfect crystalline order. The only defects seen are dislocations that can be identified as those formed during crystallization, characterized by large Burgers vectors.

The SEM image of side faces of pristine PE lamellae seen in Fig. 2a should be compared with the appearance of side faces of lamellae of the same PE material, but subjected to uniaxial compression, seen in the SEM micrograph presented in Fig. 2b. The etched side faces of heavy sheared lamellae demonstrate a fine striated texture with multiple parallel lines running across the lamellae thickness and spanning the basal lamellae planes. We

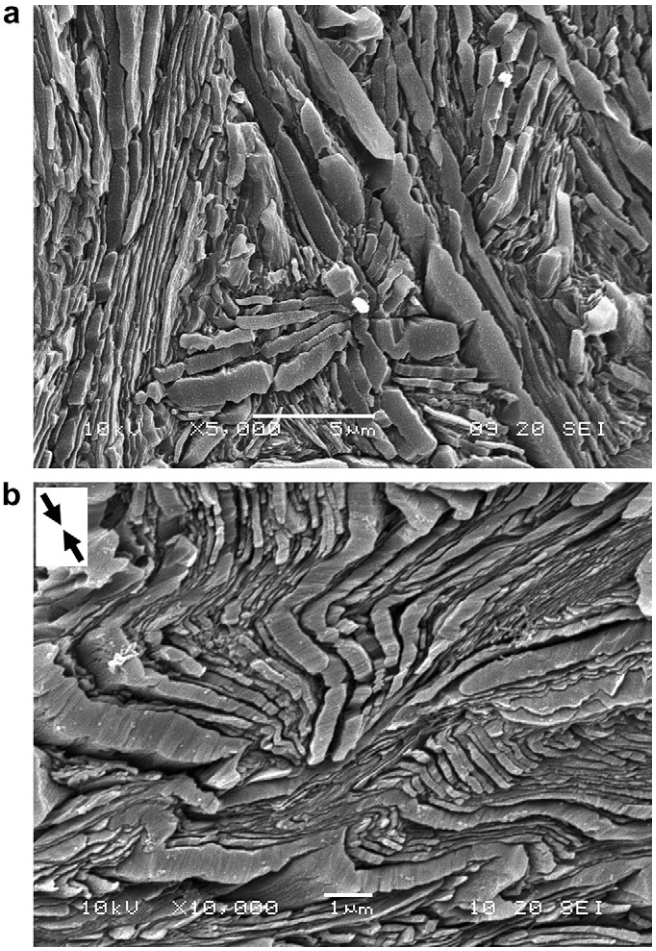

Fig. 2. SEM micrograph of bulk HDPE crystallized at high pressure of $p = 488$ MPa and $T = 247$ °C. The surface exposed by microtoming with a glass knife and etched. (a) undeformed sample, (b) sample deformed to the true strain, $e = 1.16$ (compression ratio of 3.175) with the constant true strain rate 0.005 s^{-1}. The initial crystallinity was 94.5%, mean crystal thickness $l^* = 156$ nm (from DSC melting peak).

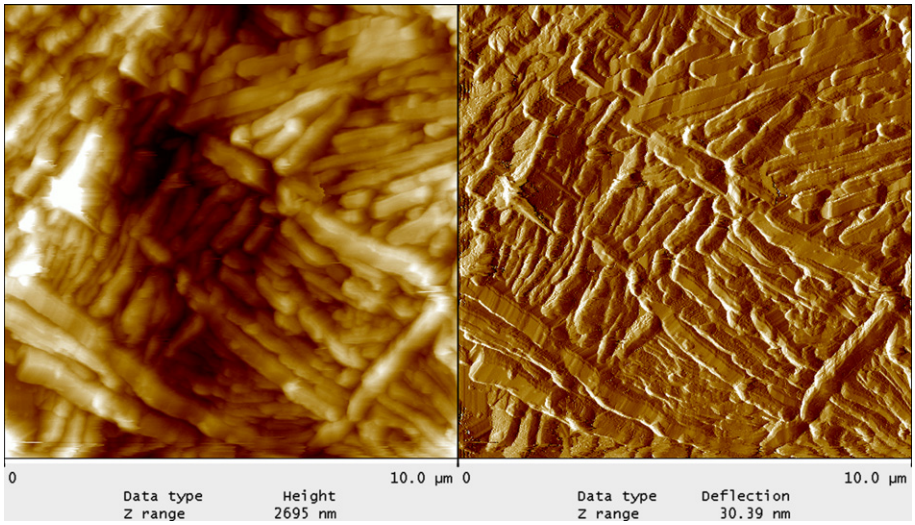

Fig. 3. AFM image of polyethylene sample compressed to the compression ratio 3.1 (true strain, $e = 1.13$) with the compression rate 0.011 s^{-1}, sectioned with AFM diamond knife and etched prior to AFM observation. Sample was crystallized at $p = 480$ MPa at $T = 235$ °C, its crystallinity was 85% and mean crystal thickness was $l^* = 97$ nm (from DSC melting peak).

attribute these lines to etched edges of screw dislocations which were generated during deformation and traveled across the crystals under the action of shear component of the stress.

Similar image of edges of sheared lamellae with numerous dislocation lines can be recognized in the AFM image of another deformed PE sample presented in Fig. 3. The number of dislocation lines per 1 µm of lamellae length can be estimated roughly at around 100. That number amounts to the concentration of about 10^{16} m^{-2} of dislocations arrested in plastically deformed PE lamellae. The above estimation agrees quite well with values reported in the literature: on the basis of theoretical considerations Seguela et al. [35] estimated an upper limit of the dislocation density as 3×10^{18} m^{-2}. Dislocation densities between 2×10^{16} and 2.2×10^{17} m^{-2} were recently determined experimentally from x-ray diffraction profile analysis in plastically deformed polypropylene [14]. Similar work for poly(3-hydroxybuthyrate) resulted in higher density of dislocations of the order of 10^{18} m^{-2} [20].

Analysis of the microscopic images of uniaxially compressed samples, as those presented in Figs. 2b and 3, including correlation between the direction of compression (marked with arrows in Fig. 2b), orientation of lamellae and orientation of dislocation lines, allows to draw the following conclusions:

1. Lamellae oriented initially along the compression direction undergo kinking. Lamellae of others orientation as well as reoriented sections of lamellae between just formed kinks undergo an intensive shear.
2. Both sheared lamellae and dislocation lines tend to assume orientation in the plane perpendicular to the compression direction. Since the screw dislocations have their Burgers vector parallel to the direction of macromolecular chain, the striation lines seen on Figs. 2b and 3 indicate the chain direction in crystals. Thus, the preferred direction of chains tends to rotate away of the compression direction.
3. Rotation of lamellae can be described by the rotation of the lamella normals towards compression direction. The simultaneous rotation of the lamella normal and chain direction in opposite directions (towards and away of compression direction, respectively) is a clear signature of the activity of the fine crystallographic slip as a primary deformation mechanism [54].
4. It is evident that the deformed polyethylene crystals are full of arrested screw dislocations and they differ significantly in crystallographic perfection from non-deformed polyethylene crystals.

According to the theory of crystal plasticity the number of dislocations taking part in deformation depends on the rate of deformation: the faster deformation the more dislocations are generated at crystal edges and travel across the crystals. Hence, crystals deformed at a higher rate should contain more dislocations that become frozen in when deformation was interrupted. One may expect then that more defected crystals ought to exhibit lower heat of melting. In fact a polyethylene sample having 81% of crystallinity with mean crystal thickness of 20 nm ($T_m = 132$ °C, $\Delta h_f = 227.2$ J/g; sample crystallized at $p = 620$ MPa and $T = 237$ °C) deformed by uniaxial compression to the true strain of 0.8 (compression ratio 2.2) with the strain rates of 0.0005, 0.005 and 0.05 s^{-1} consumes the heat of 224.6, 219.5 and 217.4 J/g during melting, respectively. The undeformed sample requires 227.2 J/g for melting. These results indicate that dislocations contribute to melting and to the

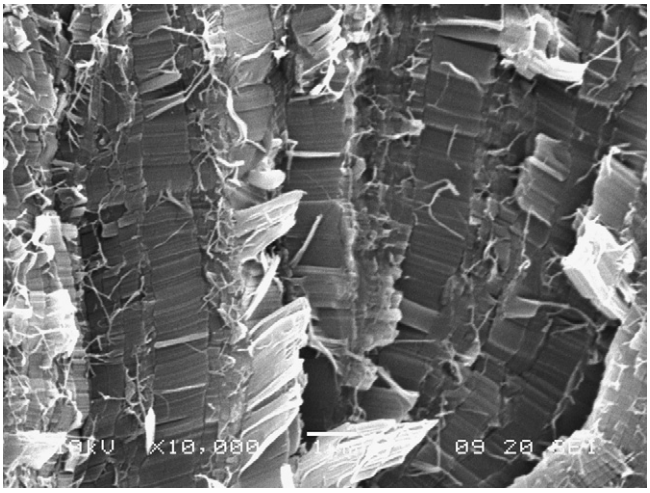

Fig. 4. SEM image of the fracture plane of undeformed PE (crystallized at $p = 480$ MPa and $T = 247$ °C), fractured at the liquid nitrogen temperature. Sample non-etched, gold coated.

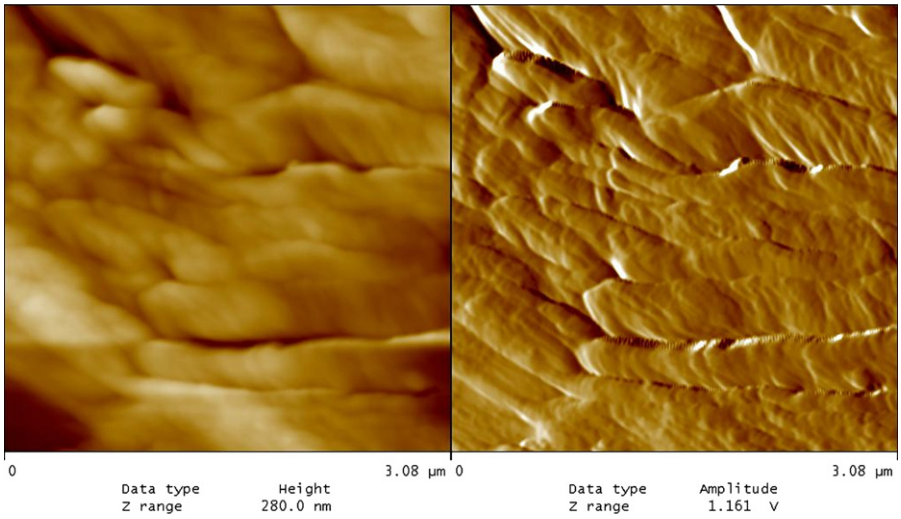

Fig. 5. Exemplary AFM image of pressure-crystallized HDPE sectioned with AFM diamond knife at $T = -160$ °C.

energy of crystals, though not very significantly. That observation agrees with the calculations performed by Young et al. [34] and Guiu et al. [30,37], who demonstrated that the generation of screw dislocations in a polymer crystal can occur under a moderate stress and the process is thermally activated.

Similar DSC measurement for a polyethylene sample with thicker crystals, 79 nm, and higher crystallinity of 93.5% ($T_m = 141.8$ °C, $\Delta h_f = 274.2$ J/g; sample crystallized at $p = 488$ MPa and $T = 242$ °C) delivered nearly identical heat of melting for deformed and undeformed material: $\Delta h_f = 273.7$ J/g, 273.6 J/g, 273.3 J/g, 273.6 J/g, and 274.2 J/g for the strain rates of 0.0005 s^{-1}, 0.005 s^{-1}, 0.05 s^{-1}, 0.5 s^{-1} and 0 (undeformed material), respectively. The uncertainty of the data is ±0.2 J/g. These results are in agreement with the rigorous energy calculations presented by Argon et al. [55] for generation of dislocation by half-loops from edges of polyethylene thick crystals. It was shown that it is relatively easy to generate and relocate the full screw dislocations in polyethylene crystals especially for thick crystals and a low temperature by the mechanism of half-loop dislocations from crystal edges.

Comparing the melting behavior of samples containing thin or thick lamellae one can conclude that the arrested dislocations contribute more to the surface energy of lamellae basal planes rather than to the bulk energy. Since the surface energy contribution is more significant in thinner than in thicker lamellae, the samples containing thin lamellae show a weak dependence of the heat of fusion on density of dislocation, controlled by the strain rate while samples with thick lamellae practically do not show that dependence.

The SEM image of the cryo-fractured PE undeformed sample (not etched), is shown in Fig. 4. Thick lamellar crystals oriented edge-on can be distinguished in this micrograph. All lamellae seen on the image exhibit a striated morphology on their side faces. Elongated peels and fibrils emanate from thin amorphous layers between lamellae. All these features indicate significant plastic deformation that occurred during cryo-fracture of PE material. That might seem somewhat strange because the sample was fractured at $T = -196$ °C (being still immersed in the liquid nitrogen), at which the amorphous component was expected to be in a glassy state and exhibit an exclusively brittle behavior (the lowest value of the glass transition temperature of PE reported in the literature is $T_g = -125$ °C). Very similar features of cryo-fractured pressure-crystallized PE were documented long time ago by Geil and Wunderlich [56]: striated morphology of side faces of chain extended lamellae, separated fibrils and plastically distorted amorphous layers between crystalline lamellae. Apparently polyethylene crystals and amorphous phase are capable of plastic deformation to some extent even at the liquid nitrogen temperature.

Another proof of such feature of polyethylene comes from results of cutting of PE by cryo-ultramicrotome equipped with a diamond knife at $T = -160$ °C. The profile of the diamond knife used (Diatome) was designed to expose the internal structure of polymeric samples for AFM microscopy. All AFM images, collected for several different samples of PE illustrate the plastic deformation on the cutting plane, which had to occur during cutting at $T = -160$ °C. An exemplary AFM image of such sample is presented in Fig. 5. It must be noted here however, that the ability of polyethylene crystals to extensive plastic deformation by crystallographic slip, even at liquid nitrogen temperature, was demonstrated in the past [57]. Therefore, numerous striations observed at the fracture surface of PE crystals can be interpreted as a result of plastic deformation of crystals by crystallographic slip, governed by generation of a great number of screw dislocations with Burgers vector along the chain direction. Deformation of the amorphous material of intercrystalline layers might be also possible at these conditions owing to local self-heating of the material within amorphous strands to the temperature above T_g.

4. Conclusions

High-pressure-crystallized PE lamellae contain low concentration of detectable screw dislocation with large Burgers vectors, estimated as $1–3 \times 10^6$ m^{-2}. Dislocations with low Burgers vectors most probably diffused outside the crystals due to annealing during long crystallization under pressure. Screw dislocations are oriented with their Burgers vectors along the chain direction and protrude across the thickness of lamellae. When etched PE lamellae are examined in the edge-on position a segmented lamellae image appear, implying a “blocky architecture” of a polymer lamellae, observed earlier by Hugel, Strobl and Thomann [51]. However, when viewed flat-on the same lamellae appear as a continuous plates with occasional screw dislocations protruding the plate. The holes left after etching of the material around dislocations lead to the false impression of lamellae composed of separated blocks, when viewed edge-on.

SEM images of deformed samples show plenty of thin lines running across deformed lamellae. We attribute those lines to

screw dislocations with low Burgers vectors that were arrested within lamellae when the deformation was interrupted. An estimated density of these dislocation is of the order of 10^{16} m^{-2}. The above conclusions fully agree with the concept of crystal plasticity governed by mobile dislocation that are generated at crystal edges. Due to numerous dislocations arrested the deformed polyethylene crystals possess lower perfection as compared with undeformed crystals, however, the volume of those crystals is nearly retained. Deformed polyethylene crystals melt at a similar T_m as undeformed crystals. Thin deformed crystals require heat of melting that is slightly dependent on the strain rate, decreasing with increasing strain rate. On contrary, thick crystals deformed with various strain rates melt at a similar temperature and with similar heat of melting within the experimental error. It suggests that the arrested dislocations contribute more to the surface energy of lamellae basal planes than to a bulk energy. Because the surface energy contribution to the heat of fusion is more significant in thin than in thick lamellae, the samples containing thin lamellae show a weak dependence of the heat of fusion on the density of dislocation, which in turn depends on the strain rate, while samples with thick lamellae practically do not show that dependence.

Polyethylene exhibits significant plasticity of both amorphous and crystalline phases way down below its T_g, as it follows from cryo-fracture and cryo-sectioning experiments. Because of that morphology of cryo-fractured lamellae is similar to that observed in samples which underwent plastic deformation: side faces of lamellae in both deformed and cryo-fractured samples demonstrate numerous striations, which may be interpreted as marks of the crystallographic slips driven by screw dislocations.

Acknowledgement

The statutory fund of the Centre of Molecular and Macromolecular Studies, Polish Academy of Sciences and Polish-Czech Academies of Sciences Bilateral Agreement are acknowledged.

References

[1] Burton WK, Cabrera N, Frank FC. Nature 1949;163:398–9.
[2] Frank FC. Discuss Farad Soc 1949;5:48–54.
[3] Honeycomb RWK. Plastic deformation of metals. London: Edward Arnold Ltd; 1968. p. 41–7.
[4] Basset DC, Keller A. Phil Mag 1962;7:1553–84.
[5] Barnes WJ, Price FP. Polymer 1964;5:283–92.
[6] Keller A. Kolloid ZZ Polymere 1967;219:118–31.
[7] Geil PH. Polymer single crystals. New York: Interscience; 1963.
[8] Wunderlich B. Macromolecular physics, crystal structure, morphology, defects. New York: Academic Press; 1973 [Chapter 4.1.4].
[9] Petermann J, Gleiter H. Phil Mag 1972;25:813–6.
[10] Petermann J, Gohil R. Polymer 1979;20:596–8.
[11] Zhou J, Li L, Lu J. Polymer 2006;47:261–4.
[12] Franke M, Rehse N. Macromolecules 2008;41:163–6.
[13] Keith HD, Chen WY. Polymer 2002;43:6263–72.
[14] Wilhelm H, Paris A, Schafler E, Bernstorff S, Bonarski J, Ungar T, et al. J Mater Sci Eng A 2004;387–389:1018–22.
[15] Schultz JM, Kinloch DR. Polymer 1969;10:271–8.
[16] Duan Y, Zhang Y, Yan S, Schultz JM. Polymer 2005;46:9015–21.
[17] Toda A, Arita T, Hikosaka M. Polymer 2001;42:2223–33.
[18] Ikehara T, Jinnai H, Kaneko T, Nishioka H, Nishi T. J Polym Sci Polym Phys Ed 2007;45:1122–5.
[19] Toda A, Okamura M, Hikosaka M, Nakagawa Y. Polymer 2005;46:8708–16.
[20] Spieckermann F, Wilhelm H, Schafler E, Kerber M, Bernstorff S, Zehetbauer MJ. 15th International conference on the strength of materials, Dresden, Germany; Aug.16–21, 2009
[21] Frank FC. Acta Crystallogr 1951;4:497–501.
[22] Keith HD, Passaglia EJ. Res Natl Bur Stand (US) 1964;68A:513–8.
[23] Young RJ. Philos Mag 1976;30:85–94.
[24] Young RJ. Mater Forum 1988;11:210–6.
[25] Lin L, Argon AS. J Mat Sci 1994;29:294–323.
[26] Seguela R. e-Polymers; 2007. Art. No: 032.
[27] Oleinik EF. Polym Sci Ser C 2003;45:17–117.
[28] Peterson JM. J Appl Phys 1966;37:4047–50.
[29] Peterson JM. J Appl Phys 1968;39:4920–8.
[30] Shadrake LG, Guiu F. Philos Mag 1976;34:565–81.
[31] Kazmierczak T, Galeski A, Argon AS. Polymer 2005;46:8926–36.
[32] Crist B, Fisher CJ, Howard P. Macromolecules 1989;22:1709–18.
[33] Darras O, Séguéla R. J Polym Sci Part B Polym Phys 1993;31:759–66.
[34] O'Kane WJ, Young RJ, Ryan AJ. J Macromol Sci Phys 1995;34:427–58.
[35] Seguela R. J Polym Sci Part B Polym Phys 2002;40:593–601.
[36] Brooks NWJ, Mukhtar M. Polymer 2000;41:1475–80.
[37] Shadrake LG, Guiu F. Philos Mag 1979;39:785–96.
[38] Bacon DJ, Tharmalingam K. J Mater Sci 1983;18:884–93.
[39] Hull D, Bacon DJ. Introduction to dislocations. 3rd ed. Oxford: Pergamon Press; 1984.
[40] Anderson FR. J Appl Phys 1964;35:64–74.
[41] Wunderlich B, Melillo L. Macromol Chem 1968;118:250–64.
[42] Prime RB, Wunderlich B. J Polym Sci A 2 1969;7:2061–97.
[43] Rees DV, Bassett DC. J Polym Sci A 2 1971;9:385–406.
[44] Bassett DC. Polymer 1976;17:460–70.
[45] Olley RH, Hodge AM, Bassett DC, Thomson JJ. J Polym Sci Polym Phys Ed 1979;17:627–43.
[46] Freedman AM, Bassett DC, Vaughan AS, Olley RH. Polymer 1986;27:1163–9.
[47] Hoffman JD. Polymer 1983;24:3–26.
[48] Hoffman JD. Polymer 1982;23:656–70.
[49] Wunderlich B, Czornyj G. Macromolecules 1977;10:906–13.
[50] Psarski M, Piorkowska E, Galeski A. Macromolecules 2000;33:916–32.
[51] Hugel T, Strobl G, Thomann R. Acta Polym 1999;50:214–7.
[52] Hippler T, Jiang S, Strobl G. Macromolecules 2005;38:9396–7.
[53] Lin L, Argon AS. Macromolecules 1994;27:6903–14.
[54] Young RJ, Bowden PB, Ritchie JM, Rider JG. J Mater Sci 1973;8:23–36.
[55] Argon AS, Galeski A, Kazmierczak T. Polymer 2005;46:11798–805.
[56] Geil P, Wunderlich B. J Polym Sci A 1964;2:3707–20.
[57] Gleiter H, Argon AS. Philos Mag 1971;24:71–80.